Effect of growth rate on the composition fluctuation of In Ga As N Ga As single quantum wells

J. F. Chen, R. S. Hsiao, P. C. Hsieh, J. S. Wang, and J. Y. Chi

Citation: Journal of Applied Physics **99**, 123718 (2006); doi: 10.1063/1.2209092
View online: http://dx.doi.org/10.1063/1.2209092
View Table of Contents: http://scitation.aip.org/content/aip/journal/jap/99/12?ver=pdfcov
Published by the AIP Publishing

Effect of growth rate on the composition fluctuation of InGaAsN/GaAs single quantum wells

J. F. Chen,[a] R. S. Hsiao, and P. C. Hsieh
Department of Electrophysics, National Chiao Tung University, Hsinchu, Taiwan 30050, Republic of China

J. S. Wang
Department of Physics, Chung Yuan Christian University, Chung-Li, Taiwan 30050, Republic of China

J. Y. Chi
Industrial Technology Research Institute (OES/ITRI), Hsinchu, Taiwan 30050, Republic of China

(Received 18 January 2006; accepted 19 April 2006; published online 29 June 2006)

Effect of growth rate on the composition fluctuation is investigated in $In_{0.34}Ga_{0.66}As_{0.98}N_{0.02}$/GaAs single quantum wells (QWs) by photoluminescence (PL), transmission electron microscopy, and admittance spectroscopy. In an InGaAsN layer grown at a normal growth rate, the PL spectra show a low-energy bump at the tail of an InGaAsN emission, suggesting the presence of composition fluctuation. Lowering the growth rate degrades the composition fluctuation by segregating into bimodal phases of an InGaAsN and InGaAs-rich phase. Further lowering the growth rate leads to a three-dimensional growth and enhances the InGaAs-rich phase. The carrier distribution for the InGaAsN layer grown at the normal rate shows a carrier bump at the tail of a strong accumulation peak, suggesting the presence of an electron state below the QW ground state. The admittance spectroscopy shows that the activation energy (32 meV) of this electron state is comparable to the energy separation (30 meV) between the InGaAsN emission and the low-energy bump, and thus it is possible that the composition fluctuation actually induces an electron state closely below the QW ground state. © *2006 American Institute of Physics*. [DOI: 10.1063/1.2209092]

I. INTRODUCTION

Recently, InGaAsN/GaAs quantum wells (QWs) have attracted considerable attention[1–10] for the realization of long wavelength optoelectronic devices. Lasers made of this material system emitting at 1.3 or 1.55 μm have been demonstrated.[2–7] However, incorporation of N considerably degrades the photoluminescence (PL) efficiency[6,8] probably due to composition fluctuation. The properties of the composition fluctuation in this material system have been studied by PL,[11–14] transmission electron microscopy (TEM),[14] and deep-level transient spectroscopy (DLTS).[15–17] Despite these efforts, little is known about the detailed relationship between composition fluctuation and growth conditions[18] and the effect of composition fluctuation on the electrical properties. Furthermore, although optical states induced by composition fluctuation were previously reported in AlGaAs–GaAs QW structures,[19] to the authors' knowledge, electrical states induced by composition fluctuation has seldom been investigated. Therefore, in this paper, we continue this study by varying the InGaAsN deposition rate in InGaAsN/GaAs single quantum wells (SQWs) and characterized their PL, structural and electrical properties. The electrical properties were characterized by frequency-dependent capacitance-voltage (*C-V*) and admittance spectroscopy. We show that lowering the growth rate degrades composition fluctuation by segregating into bimodal phases of an InGaAsN and an InGaAs-rich phase. The carrier distribution and emission studies show that composition fluctuation actually introduces an electron confinement state closely below the InGaAsN electron ground state.

II. EXPERIMENTS

The samples were grown on n^+-GaAs (001) substrates by molecular beam epitaxy. An EPI-Unibulb radio frequency (rf) plasma source was used to provide nitrogen species from a pure N_2 gas. The indium and gallium were supplied from conventional Knudsen effusion cells, and As in the form of As_2 were supplied from a cracker source. A 0.3 μm Si-doped GaAs layer of $\sim 6\times 10^{16}$ cm^{-3} was first grown at 580 °C, followed by a 60 Å thick InGaAsN layer with 2% N composition, grown at 420 °C. The InGaAsN layers grown at this temperature are high quality and emit at 1.3 μm.[20] Too low a growth temperature increases defects or impurity incorporation and too high a growth temperature may lead to phase separation[12] and poor surface morphology. Detailed relationship between the quality of the InGaAsN layers and growth temperatures has been established.[21] After the growth of the InGaAsN layer, a 0.3 μm Si-doped GaAs layer of $\sim 6\times 10^{16}$ cm^{-3} was grown to terminate the whole structure. The In and Ga cell temperatures were controlled to yield a 34% In and 66% Ga composition. The growth rates of the InGaAsN layer were varied by scaling the In and Ga fluxes. The N composition of 2% is determined by x-ray diffraction combined with x-ray dynamic simulation. Based on the experimental emission energy of the InGaAsN layer, the room-temperature band-gap energy of the InGaAsN layer was es-

[a]Electronic mail: jfchen@cc.nctu.edu.tw

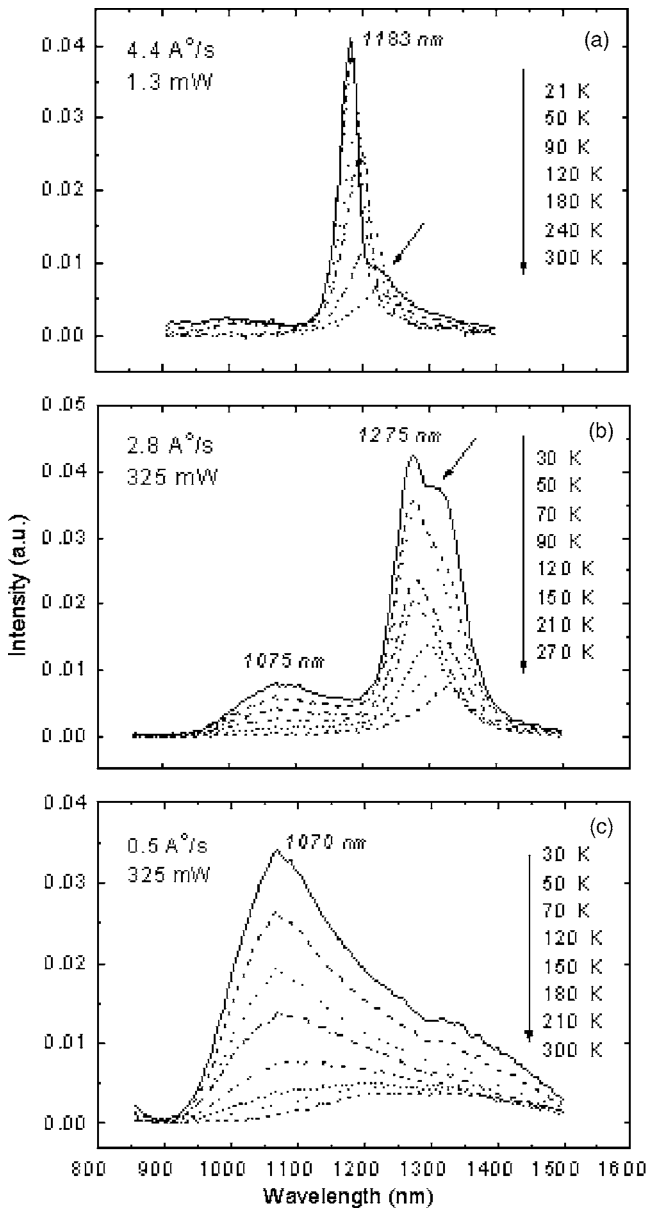

FIG. 1. Temperature-dependent PL spectra for the InGaAsN layers grown at deposition rates of (a) 4.4, (b) 2.8, and (c) 0.5 Å/s, respectively. The 4.4 Å/s sample displays an InGaAsN emission and a low-energy bump (indicated by an arrow) due to composition fluctuation. The 2.8 Å/s sample displays bimodal phase segregation of an InGaAsN phase with a low-energy shoulder (indicated by an arrow) and an InGaAs-rich phase at around 1075 nm. Further lowering the growth rate to 0.5 Å/s enhances the InGaAs-rich phase.

timated to be about 0.9 eV. Schottky contacts were fabricated by evaporating Al with a dot diameter of 800 μm. PL spectra were obtained by a frequency doubled (yttrium aluminum garnet) YAG:Nd laser (λ=532 nm) and an InGaAs detector. An HP 4194A impedance analyzer was used to perform admittance spectroscopy.

III. RESULTS AND DISCUSSIONS

A. Effect of composition fluctuation on PL spectra

Figures 1(a)–1(c) show the temperature-dependent PL spectra for the InGaAsN layers deposited at 4.4, 2.8, and 0.5 Å/s, respectively, under a laser power of 1.3 mW (325 mW) for the 4.4 Å/s sample (2.8 and 0.5 Å/s samples). The 4.4 Å/s sample emits at 1265 nm (at 300 K) with a narrow linewidth of 20 meV (at 21 K). However, when temperature is lowered, a tail emerges on the low energy side. Similar low-energy tails were observed in N–As alloys and were attributed to the recombination of excitons trapped by localized states at the band tails[13] induced by inevitable composition fluctuation. The absence of this tail at high temperatures is due to the trapped photocarriers thermally activating from the localized states to delocalized states. This tail suggests the presence of composition fluctuation which is inevitable for high N content. When temperature decreases to 21 K, the low-energy tail becomes a bump (as indicated by an arrow) with an energy separation of about 30 meV from the main emission. This bump suggests the presence of local regions with a higher N composition than the average, i.e., N clusters.

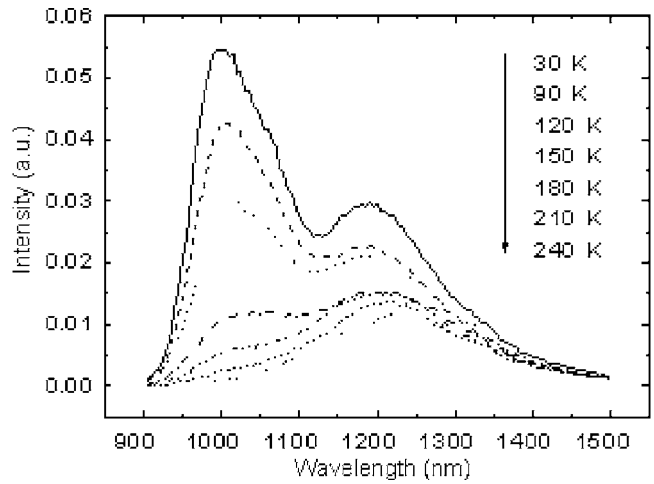

FIG. 2. PL spectra of a GaAs/$In_{0.34}Ga_{0.66}As$/GaAs structure. The emission spectra at 1000 nm and its temperature dependence are similar as that of the InGaAs-rich phase in Fig. 1(c). The weak emission at 1200 nm originates from the impurities or defects in the GaAs substrate.

Lowering the growth rate to 2.8 Å/s causes a slight redshift of the InGaAsN emission (to 1330 nm at 300 K) presumably due to an increased N content since only In and Ga fluxes are scaled down. Lowering the growth rate degrades the InGaAsN emission but enhances the low-energy tail which becomes a pronounced shoulder (indicated by an arrow) with comparable intensity as the InGaAsN emission. Note that their energy separation remains nearly the same as that in the 4.4 Å/s sample. Additionally, the PL spectra clearly display a very broad spectrum around 1075 nm. The corresponding energy is about 0.2 eV larger than that of the InGaAsN emission, and thus this broad spectrum cannot be attributed to defect states induced within the band gap of the InGaAsN layer. By comparison, we found that this broad spectrum is similar to that of InGaAs/GaAs QW structures grown at our laboratory. Figure 2 shows the PL spectra (under a laser power of 13 mW) of a 600 Å GaAs/60 Å $In_{0.34}Ga_{0.66}As$/GaAs structure. The emission at ~1000 nm is due to the InGaAs layer and the weak emission at 1200 nm originates from the impurities or defects in the GaAs substrate because a back-side illumination shows such a similar emission. The similarity between the broad spectrum and the

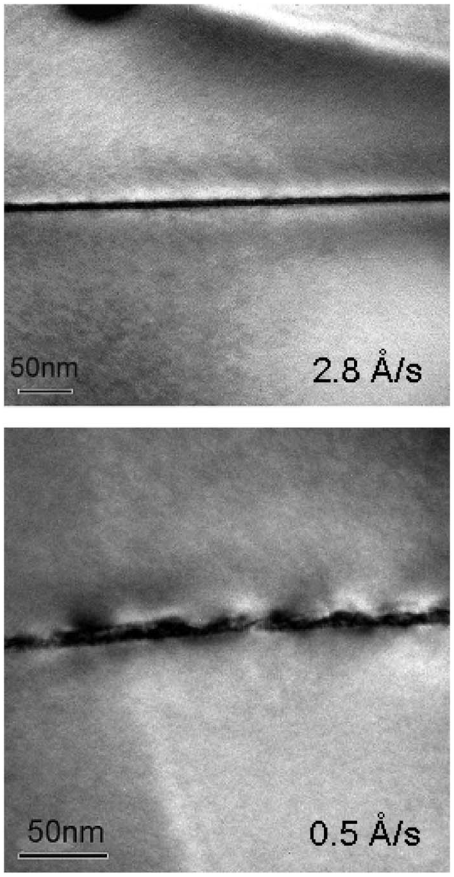

FIG. 3. Images of cross-sectional TEM pictures of the 2.8 and 0.5 Å/s samples, respectively. In contrast to the flat interfaces in the 2.8 Å/s sample, the 0.5 Å/s sample shows undulated interfaces with dark regions.

InGaAs emission suggests the presence of local regions where the N composition may be depleted, which will be referred as an InGaAs-rich phase. Thus, lowering the growth rate may segregate into bimodal phases of an InGaAsN phase and an InGaAs-rich phase.

Further lowering the growth rate to 0.5 Å/s leads to the PL spectra [Fig. 1(c)] that are dominated by the InGaAs-rich phase. The intensity of this phase rapidly decreases with increasing temperature. This temperature dependence can be attributed to a weaker confining potential for InGaAs in GaAs as indicated by its wavelength, in comparison with the InGaAsN emission. Note that the InGaAs-rich phase shows similar temperature dependence as the InGaAs emission in Fig. 2, further supporting the assignment. The enhancement of the InGaAs-rich phase is related to a three-dimensional (3D) growth mode observed in this sample, as suggested by spotty patterns of reflection high-energy electron diffraction (RHEED). Figure 3 shows the cross-sectional TEM images of the 2.8 and 0.5 Å/s samples. While the 2.8 Å/s sample shows relatively flat interfaces, the 0.5 Å/s sample shows rather undulated interfaces with small dark regions like dots. These dotlike states destroy the size-quantization effect, leading to the severely degraded InGaAsN emission. Figure 4 shows the PL spectra of the 0.5 Å/s sample after a rapid thermal annealing at 800 °C for 5 min. By comparison with the spectra before annealing in Fig. 1(c), the annealing significantly recovers the InGaAsN emission and suppresses the InGaAs-rich emission. This result indicates that annealing can reduce composition fluctuation, consistent with previous result.[14]

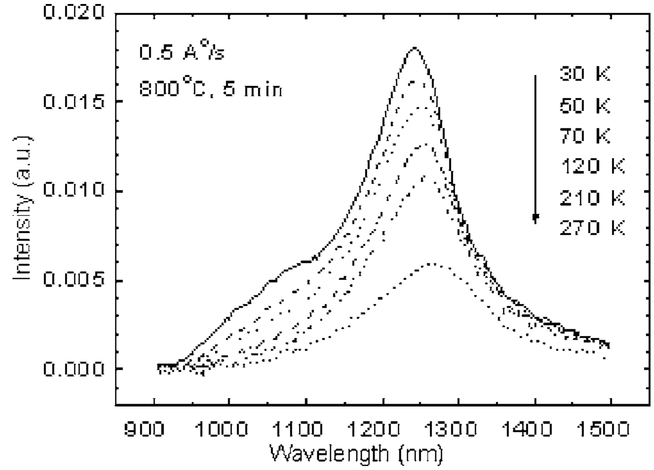

FIG. 4. The PL spectra of the 0.5 Å/s sample after a postgrowth annealing at 800 °C for 5 min. Recovery of the InGaAsN phase and suppression of the InGaAs-rich phase can be seen.

B. Effect of composition fluctuation on carrier distribution

As shown, the 0.5 Å/s sample shows 3D growth mode and the 2.8 Å/s sample shows bimodal phase segregation. The induced defects may be too complicated or could be avoided by increasing the growth rate. The 4.4 Å/s sample shows high quality, but still contains composition fluctuation as indicated by the low-energy PL bump. DLTS measurements have performed on this sample and found no defect traps, indicating that such minor composition fluctuation does not induce any deep levels. The effect of the composition fluctuation on the carrier distribution is shown in Fig. 5,

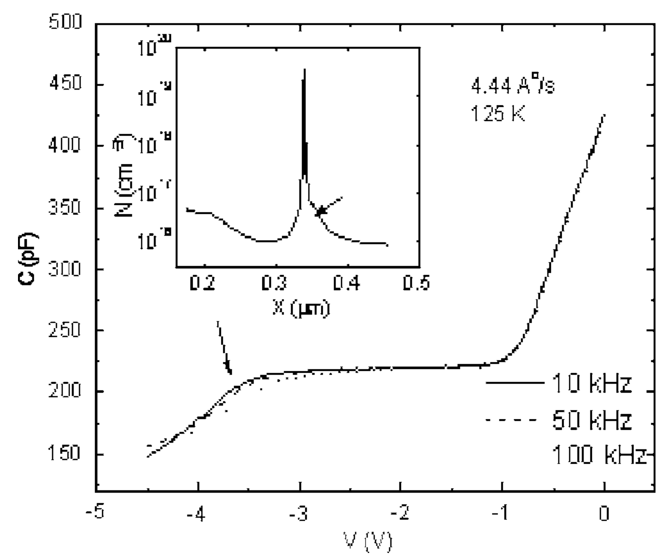

FIG. 5. The *C-V* spectra at 125 K and the carrier distribution (in the inset) of the 4.4 Å/s sample. A *C-V* plateau followed by capacitance dispersion over frequency at around −3.5 V (indicated by an arrow) can be seen. The dispersion suggests the presence of an electron state closely below the InGaAsN electron ground state.

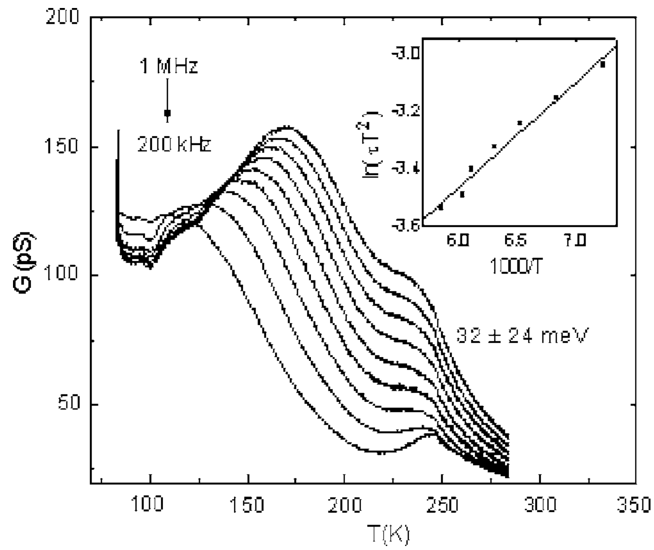

FIG. 6. The frequency-dependent *G-T* spectra of the 4.4 Å/s sample, measured at −3.5 V. A peak at ~150 K and a weak shoulder at ~230 K can be seen. The weak bump originates from a geometric *RC* time constant effect. The peak at ~150 K corresponds to the frequency dispersion of the carrier bump in Fig. 5. The inset shows the Arrhenius plots of the emission times of the peak at ~150 K, which yield an activation energy of 32±24 meV.

where *C-V* spectra and the corresponding carrier profile (in the inset) are shown. A capacitance plateau and its corresponding carrier peak is visible due to the electron accumulation in QW ground state. The intensity of this peak increases with decreasing temperature, characteristic of a Debye-length effect in quantum structures. No attenuation of this peak is seen up to 1 MHz at 10 K, suggesting that the emission from the ground state in the well to the GaAs electrode is less than 10^{-6} s at 10 K, which cannot be resolved under available frequency. As shown in the inset of this figure, this peak is followed by a weak bump (indicated by an arrow), which corresponds to the capacitance dispersion over frequency at −3.5 V. This bump suggests the presence of a state and the dispersion is due to the inability of the electrons to follow ac modulating signal to emit from this state. As shown, this bump can follow ac signal at 10 KHz but cannot at 100 KHz. From the middle frequency (50 KHz), the emission time τ is $\sim 2\times 10^{-5}$ s (at 125 K). Accurate emission times and their temperature dependence can be obtained by the conductance-temperature (*G-T*) spectra, measured at −3.5 V, as shown in Fig. 6. Each curve displays a dominant peak at around 150 K and a weak shoulder at around 230 K. The weak bump shows nearly no temperature dependence and is identified to originate from the geometric resistance-capacitance (*RC*) time constant effect and thus is no interest to us. The low-temperature peak corresponds to the carrier bump due to their similar emission times. A peak appears when frequency is comparable to the emission rate, according to the relation $2\pi f\tau \cong 2$. The peak shifts to a higher temperature for a higher frequency, reflecting a reduction of the emission time with increasing temperature. The Arrhenius plots of the emission times, as shown in the inset of Fig. 6, yield an activation energy (capture cross section) of 32 ± 24 meV (1.3×10^{-18} cm^2). This activation energy slightly increases with increasing magnitude of the reverse bias, suggesting that the state is not very sharp in energy. From these results, we conclude that there exists an electron state at 32 meV below the electron ground state of the InGaAsN well. When applying a modulating signal, electrons are activated from this state to the InGaAsN ground state and subsequently activated to the bottom GaAs electrode. Only the emission time for the former process is obtained since the latter process has an emission time less than 10^{-6} s at 10 K and is too fast to be resolved.

In terms of its energy location, this electron state may be responsible for the observed PL low-energy bump due to composition fluctuation. Figure 1(a) shows that the low-energy bump is separated from the InGaAsN emission by about 30 meV which is comparable to the activation energy of this electron state. Based on this consistency, it is possible that the composition fluctuation actually forms an electron state at 32 meV below the InGaAsN electron ground state. Formation of such a state will influence the carrier distribution and electron emission from the QW states. Finally, it may be worth mentioning that the emission properties of the electron state, including its carrier distribution and the *G-T* spectra, are similar to that observed in InAs quantum dots.[22] This similarity suggests that the InGaAsN layer grown at 4.4 Å/s may contain N clusters whose size is too small to be observed in TEM. This argument is supported by the observation of dotlike states in the growth of InGaAsN/GaAs QWs after annealing.[14]

IV. CONCLUSIONS

In summary, we have investigated the effect of deposition rate on the composition fluctuation in InGaAsN/GaAs single quantum wells. In an InGaAsN layer grown at 4.4 Å/s, PL spectra show an additional low-energy bump due to composition fluctuation. The carrier distribution of this sample shows a carrier bump at the tail of a strong accumulation peak, suggesting the presence of an electron state. Admittance spectroscopy shows that the electron state has an activation energy comparable to the energy separation between the InGaAsN emission and the low-energy bump. Accordingly, the composition fluctuation may induce an electron state closely below the InGaAsN electron ground state. Lowering the growth rate to 2.8 Å/s degrades the composition fluctuation by segregating into bimodal phases: an InGaAsN and an InGaAs-rich phase. Further lowering the growth rate to 0.5 Å/s leads to a 3D growth mode. Post-growth annealing at 800 °C for 5 min can recover the InGaAsN phase and suppress the InGaAs-rich phase, suggesting that annealing can effectively reduce the composition fluctuation.

ACKNOWLEDGMENTS

The authors would like to thank the National Science Council of the Republic of China, Taiwan for financially supporting this research under Contract No. NSC-94-2112-M-009-029.

[1]M. Kondow, K. Uomi, A. Niwa, T. Kitatani, S. Watahiki, and Y. Yazawa, Jpn. J. Appl. Phys., Part 1 **35**, 1273 (1996).
[2]F. Hohnsdorf, J. Koch, C. Agert, and W. Stolz, J. Cryst. Growth **195**, 391

(1998).
[3]A. Wagner *et al.*, Appl. Phys. Lett. **76**, 271 (2000).
[4]S. Sato, Y. Osawa, T. Saitoh, and I. Fujimura, Electron. Lett. **33**, 1386 (1997).
[5]M. Kondow, S. Nakatsuka, T. Kitatani, Y. Yazawa, and M. Kai, Jpn. J. Appl. Phys., Part 1 **35**, 5711 (1996).
[6]H. P. Xin and C. W. Tu, Appl. Phys. Lett. **72**, 2442 (1998).
[7]K. Nakahara, M. Kondow, T. Kitani, M. C. Larson, and K. Uomi, IEEE Photonics Technol. Lett. **10**, 487 (1998).
[8]S. R. Kurtz, A. A. Allerman, E. D. Jones, J. M. Gee, J. J. Banas, and B. E. Hammons, Appl. Phys. Lett. **74**, 729 (1999).
[9]M. Weyers, M. Sato, and H.. Ando, Jpn. J. Appl. Phys., Part 2 **31**, L853 (1992).
[10]S. Sato, Y. Osawa, and T. Saitoh, Jpn. J. Appl. Phys., Part 1 **36**, 2671 (1997).
[11]S. G. Spruytte, C. W. Coldren, J. S. Harris, P. Krispin, K. Ploog, and M. C. Larson, J. Appl. Phys. **89**, 4401 (2001).
[12]M. A. Pinault and E. Tournie, Appl. Phys. Lett. **79**, 3404 (2001).
[13]I. A. Buyanova, W. M. Chen, G. Pozina, J. P. Bergman, B. Monemar, H. P. Xin, and C. W. Tu, Appl. Phys. Lett. **75**, 501 (1999).
[14]H. P. Xin, K. L. Kavanagh, Z. Q. Zhu, and C. W. Tu, Appl. Phys. Lett. **74**, 2337 (1999).
[15]D. Kwon, R. J. Kaplar, S. A. Ringel, A. A. Allerma, S. R. Kurtz, and E. D. Jones, Appl. Phys. Lett. **74**, 2830 (1999).
[16]P. Krispin, S. G. Spruytte, J. S. Harris, and K. H. Ploog, J. Appl. Phys. **88**, 4153 (2000).
[17]R. J. Kaplar, S. A. Ringel, S. R. Kurtz, J. F. Klem, and A. A. Allerman, Appl. Phys. Lett. **80**, 4777 (2002).
[18]R. J. Kaplar, A. R. Arehart, S. A. Ringel, A. A. Allerman, R. M. Sieg, and S. R. Kurtz, J. Appl. Phys. **90**, 3405 (2001).
[19]N. Holonyak Jr., W. D. Laidig, B. A. Vojak, K. Hess, J. J. Coleman, P. D. Dapkus, and J. Bardeen, Phys. Rev. Lett. **45**, 1703 (1980).
[20]R. S. Hsiao *et al.*, Jpn. J. Appl. Phys., Part 2 **43**, L1555 (2004).
[21]J. S. Wang, A. R. Kovsh, R. S. Hsiao, L. P. Chen, J. F. Chen, T. S. Lay, and J. Y. Chi, J. Cryst. Growth **262**, 84 (2004).
[22]J. F. Chen, R. S. Hsiao, C. K. Wang, J. S. Wang, and J. Y. Chi, J. Appl. Phys. **98**, 013716 (2005).